# Numerical Simulation of Blood Flow Through the System of Coronary Arteries with diseased Left Anterior Descending

Pearanat Chuchard, Thitikom Puapansawat, Thanongchai Siriapisith, Yong Hong Wu and Benchawan Wiwatanapataphee

***Abstract*—This paper aims to study the arterial stenosis effect on blood flow problem in the system of coronary arteries. Blood is assumed to be non-Newtonian incompressible fluid. The system of coronary arteries with diseased Left Anterior Descending (LAD) is considered. Governing equations are the Navier-Stokes equations and continuity equation subjected to the time-dependent pulsatile boundary conditions. Based on finite element method, the solution of the governing equations is solved numerically. Disturbances of blood flow through the diseased LAD for the restrictions of 25%, 50% and 75% are investigated. Flow characteristics, wall pressure and wall shear rate have been studied in detail. Numerical studies show that blood flow with high speed and pressure rapidly drops in the area supplied by the stenosed artery. As the degree of coronary-artery stenosis increases, the maximal coronary flow decreases.**

***Index Terms*—blood flow, stenosed coronary artery, pulsatile boundary condition , finite element method.**

## I. Introduction

The most common form of heart disease is the coronary artery disease (CAD). Over 7 million people in developed and developing countries suffer from it. CAD is an occlusion of the coronary arteries resulting in insufficient supply of blood and oxygen deprivation to the heart muscle. When the blockage of an artery is complete, it results in a heart attack, or in very severe cases, may result in death of the patient. To overcome the problem, detailed knowledge associated with the disordered flow patterns in stenosis is then important for the detection of localized arterial disease in its early stages. In order to understand the pathogenesis of coronary diseases, a number of in-vivo and vitro experiments have been conducted using animal models [12, 14, 17, 25]. Uren et al. (1994) studied the relation between the severity of stenosis in a coronary artery and the degree of impairment of myocardial blood flow in laboratory animals. It is reported that the increasing degree of coronary-artery stenosis increases gives the maximal coronary flow. Due to the difficulty in determining the critical flow conditions for the in-vivo and vitro experiments, the exact mechanism involves is not well understood. On the other hand, mathematical modeling and numerical simulation can lead to better understanding of the phenomena involved in vascular disease [1, 5, 6, 8, 9, 11, 13, 16, 19, 20, 21, 22, 23]. Over the last two decades, a number of mathematical models and numerical techniques has been proposed to describe blood flow in a stenosed coronary artery [7, 10, 12, 15, 18]. Wiwatanapataphee (2008) [4] studied the effect of stenosed arteries in a stenosed tube with non-Newtonian model of blood. It is indicated that blood pressure drops significantly around the stenosis region. The blood pressure continuously drops as the degree of stenosis increases. Chaniotis et al. (2010) [2] studied the pulsatile blood flow in the computational geometry of coronary. The Newtonian model and non-Newtonian model were used to compare on wall shear stress distribution. Their results showed that the effect of non-Newtonian model was significant. Cheung et al. (2010) [3] studied blood flow through stenosed bifurcation vessel using experimental and numerical models. The experimental study was based on PIV measurements, while the numerical study was based on CFD simulation. They concluded that numerical

This work was supported by the Development and Promotion of Science and Technology Talents Project (DPST), the Office of the Higher Education Commission, and the Thailand Research Fund

P. Chuchard is with Department of Mathematics, Faculty of Science, Mahidol University, 272 Rama 6 Road, Rajthevee, Bangkok 10400 THAILAND (corresponding author; e-mail:g5237100@student.mahidol.ac.th).

T. Puapansawat is with Department of Mathematics, Faculty of Science, Mahidol University, 272 Rama 6 Road, Rajthevee, Bangkok 10400 THAILAND (e-mail:sctpw@mahidol.ac.th).

T. Siriapisith is with Department of Radiology, Faculty of Medicine Siriraj Hospital, Mahidol University, Bangkok, THAILAND (e-mail:thanongchai@gmail.com).

Y.H. Wu is with Department of Mathematics and Statistics, Curtin University of Technology, Perth, WA 6845 AUSTRALIA (e-mail:yhwu@maths.curtin.edu.au).

B. Wiwatanapataphee is with Department of Mathematics, Faculty of Science, Mahidol University, 272 Rama 6 Road, Rajthevee, Bangkok 10400 THAILAND (corresponding author; e-mail:scbww@mahidol.ac.th).

simulation based on an realistic geometry of human coronary arteries provided accurate result against the experiment.

Due to the fact that construction of a realistic geometry of the coronary artery system is a difficult task, a unrealistic vessel geometry including a straight tube or curve tube with branches and with no branch are used in the above mentioned studies. It has been accepted that the results that obtained from unrealistic geometry may not be appropriate for clinical use. In spite of extensive modeling studies on blood flow in the stenosed coronary artery, little work has been done to solve the blood flow problem in the system of the coronary arteries. Most studies use either the right coronary artery (RCA) or the left coronary artery (LCA) without the aorta.

In this study, we simulated the three-dimensional unsteady non-Newtonian blood flow in the system of human coronary artery with diseased LAD. The pulsatile boundary condition is considered. Effect of different degree of stenosis on the blood flow is investigated. The rest of the paper is organized as follows: Section II concerns mathematical model and finite element formulation. Numerical example is presented in section III. Conclusion is given in section IV.

## II. Mathematical Models

### A. Governing Equations

In this study, the motion of blood flow is governed by the continuity equation and Navier-Stoke equations:

$$\nabla \cdot \boldsymbol{u} = 0, \tag{1}$$

$$\frac{\partial \boldsymbol{u}}{\partial t} + (\boldsymbol{u} \cdot \nabla)\boldsymbol{u} = \frac{1}{\rho}\nabla \cdot \sigma. \tag{2}$$

where $\boldsymbol{u}$ is blood velocity, $\rho$ is blood density, $\sigma$ is the stress-deformation rate relation which is described by

$$\sigma = [-pI + \eta(\dot{\gamma})(\nabla \boldsymbol{u} + (\nabla \boldsymbol{u})^T)] \tag{3}$$

where p is blood pressure and $\eta(\dot{\gamma})$ denotes the viscosity of incompressible non-Newtonian blood determined by Carreau model [24]:

$$\eta(\dot{\gamma}) = n_\infty + (n_0 - n_\infty)[1 + (\lambda\dot{\gamma})^2]^{(n-1)/2}, \tag{4}$$

where $n_\infty$, $n_0$, $\lambda$, n are parameters and the shear rate $\dot{\gamma}$ defined by

$$\dot{\gamma} = \sqrt{2tr(\frac{1}{2}(\nabla \boldsymbol{u} + (\nabla \boldsymbol{u})^T)^2}. \tag{5}$$

To specify the pulsatile behavior of blood flow, the cyclic nature of the heart pump is considered. In this study, we assume that the cardiac cycle has no difference in time variation, the pulsatile pressure and the flow rate of blood can be expressed by the periodic functions $p(t) = p(t + nT)$ and $Q(t) = Q(t + nT)$ for $n = 0, 1, 2, ...$ and $T$ is the cardiac period. Mathematically, the pulsatile pressure $p(t)$ and flow rate $Q(t)$ can be written in the form of the truncated Fourier series:

$$\begin{aligned} p(t) &= \bar{p} + \sum_{k=1}^{4} \alpha_k^p \cos k\omega t + \beta_k^p \sin k\omega t, \\ Q(t) &= \bar{Q} + \sum_{k=1}^{4} \alpha_k^Q \cos k\omega t + \beta_k^Q \sin k\omega t, \end{aligned} \tag{6}$$

where $\bar{p}$ denotes the mean pressure, $\bar{Q}$ is the mean flow rate and $\omega = 2\pi/T$ is the angular frequency with cardiac period $T$.

On the inflow surface $\Gamma^{aorta}$ of the aorta, we enforce the pulsatile velocity condition:

$$u(t) = \frac{Q(t)}{A}, \tag{7}$$

where $A$ is the area of the inlet surface. On the outflow surface, we enforce the corresponding pulsatile pressure condition:

$$p = p_0(t), \eta(\nabla \boldsymbol{u} + (\nabla \boldsymbol{u})^T) = 0. \tag{8}$$

In summary, the blood flow in the coronary artery system is governed by the following boundary value problem (BVP):

BVP: Find $\boldsymbol{u}$ and $p$ such that equation (1)-(6) and all boundary conditions (7)-(8) are satisfied.

TABLE I
Values of the parameters $\alpha_k^Q$, $\beta_k^Q$, $\alpha_k^p$ and $\beta_k^p$ used in the formula 6

| $k$ | $\alpha_k^Q$ | $\beta_k^Q$ | $\alpha_k^p$ | $\beta_k^p$ |
|---|---|---|---|---|
| 1 | 1.7048 | -7.5836 | 8.1269 | -12.4156 |
| 2 | -6.7035 | -2.1714 | -6.1510 | -1.1072 |
| 3 | -2.6389 | 2.6462 | -1.3330 | -0.3849 |
| 4 | 0.7198 | 0.2687 | -2.9473 | 1.1603 |

### B. Finite Element Formulation

This section concerns the finite element formula. Starting with the total weighted residual of the system of equation (1-2), we obtain the variational statement corresponding to the BVP:

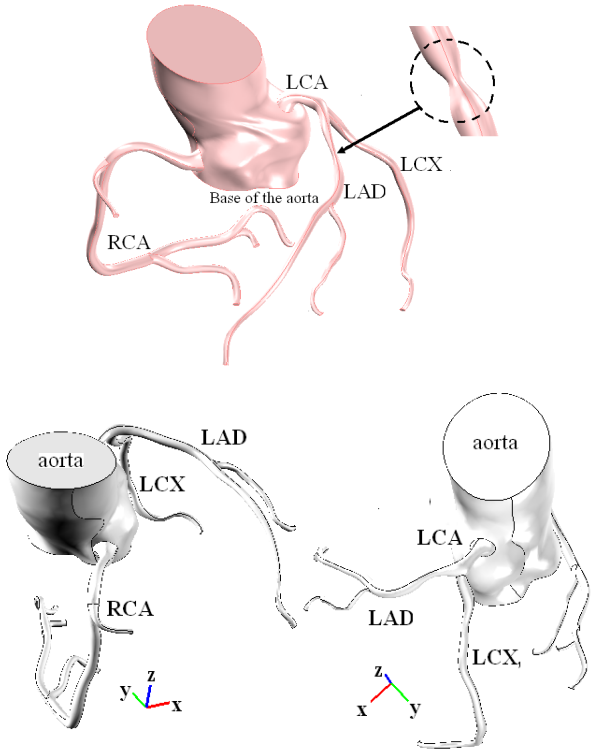


Fig. 1. The computational domain of the system of coronary arteries

Find $\boldsymbol{u}$ and $p \in H^1(\Omega)$ such that for all $\mathbf{w}^u$ and $w^p \in H_0^1(\Omega)$, all boundary conditions are satisfied and

$$(\nabla \cdot \boldsymbol{u}, w^p) = 0, \tag{9}$$

$$\begin{aligned}&(\frac{\partial \boldsymbol{u}}{\partial t}, \mathbf{w}^u) + ((\boldsymbol{u} \cdot \nabla)\boldsymbol{u}, \mathbf{w}^u) = \\ &\frac{1}{\rho}(\nabla \cdot [-pI + \eta(\nabla \boldsymbol{u} + (\nabla \boldsymbol{u})^T)], \mathbf{w}^u).\end{aligned} \tag{10}$$

where $H^1(\Omega)$ is the Sobolev space $W^{1,2}(\Omega)$ with norm $\| \cdot \|_{1,2,\Omega}$, $H_0^1(\Omega) = \{v \in H^1(\Omega) | v = 0$ on the Dirichlet type boundary$\}$ and $(\cdot, \cdot)$ denoted the inner product on the square integrable function space $L^2(\Omega)$, defined by.

$$(u, v) = \int_\Omega u \cdot v \, \mathrm{d}\Omega. \tag{11}$$

The second order derivatives in equations (9) and (10) are reduced to the first order using Green's formula. We then have

$$(\nabla \cdot \boldsymbol{u}, w^p) = 0, \tag{12}$$

$$\begin{aligned}&(\frac{\partial \boldsymbol{u}}{\partial t}, \mathbf{w}^u) + ((\boldsymbol{u} \cdot \nabla)\boldsymbol{u}, \mathbf{w}^u) \\ - \quad &\frac{1}{\rho}(\nabla w^u, [pI - \eta(\nabla \boldsymbol{u} + (\nabla \boldsymbol{u})^T)]) \\ - \quad &\frac{1}{\rho}[a(w^u, \sigma \cdot \boldsymbol{n})] = 0\end{aligned} \tag{13}$$

To solve the above problem using the Galerkin Finite Element method. For $\boldsymbol{u}$ and $w^u$, we choose an L-dimensional subspace $H_L$ of $H^1(\Omega)$ and a basis functions $\{\phi\}_{i=1}^L$ of $H_L$. We then obtain

$$\boldsymbol{u}(x,t) \approx \boldsymbol{u}_L = \sum_{\alpha=1}^{L} \boldsymbol{u}_\alpha(t)\phi_\alpha(x), \tag{14}$$

$$\mathbf{w}^u \approx (\mathbf{w}^u)_L = \sum_{\beta=1}^{L} \mathbf{w}_\beta^u(t)\phi_\beta(x). \tag{15}$$

Choosing an M-dimensional subspace $H_M$ of $H^1(\Omega)$ with a basis functions $\{\varphi\}_{i=1}^M$ for $p$ and $w^p$. We then obtain

$$p(x,t) \approx p_M = \textstyle\sum_{\gamma=1}^{M} p_\gamma(t)\varphi_\gamma(x), \tag{16}$$

$$w^p \approx (w^p)_M = \textstyle\sum_{\delta=1}^{M} w_\delta^p(t)\varphi_\delta(x), \tag{17}$$

From equations (14)-(17), replacing $\boldsymbol{u}$, $p$, $\mathbf{w}^u$ and $w^p$ in equations (12)-(13) for arbitrary $\mathbf{w}^u$, $w^p$ and applying boundary condition 8, we then have

$$\sum_{\alpha=1}^{L} (\psi_\delta, \frac{\partial \phi_\alpha}{\partial x_i}) u_{j\alpha} = 0, \tag{18}$$

$$\begin{aligned}&\sum_{\alpha=1}^{L} (\phi_\beta, \phi_\alpha)\dot{u}_{i\alpha} + \sum_{\alpha=1}^{L} (\phi_\beta, u_j \frac{\partial \phi_\alpha}{\partial x_j}) u_{i\alpha} \\ - \quad &\frac{1}{\rho}\sum_{\gamma=1}^{M} (\psi_\gamma, \frac{\partial \phi_\beta}{\partial x_i}) p_\gamma + \frac{1}{\rho}\sum_{\alpha=1}^{L} (\frac{\partial \phi_\beta}{\partial x_j}, \eta \frac{\partial \phi_\alpha}{\partial x_j}) u_{i\alpha} \\ + \quad &\frac{1}{\rho}\sum_{\alpha=1}^{L} (\frac{\partial \phi_\beta}{\partial x_j}, \eta \frac{\partial \phi_\alpha}{\partial x_i}) u_{j\alpha} = 0\end{aligned} \tag{19}$$

The system of equations (18) and (19) can be written in matrix from as

$$C_1^T U_1 + C_2^T U_2 + C_3^T U_3 = 0 \tag{20}$$

$$M \begin{bmatrix} \dot{U}_1 \\ \dot{U}_2 \\ \dot{U}_3 \end{bmatrix} + A \begin{bmatrix} U_1 \\ U_2 \\ U_3 \end{bmatrix} - \begin{bmatrix} C_1 \\ C_2 \\ C_3 \end{bmatrix} P = 0 \tag{21}$$

where

$$M = \begin{pmatrix} m_{\beta\alpha} & 0 & 0 \\ 0 & m_{\beta\alpha} & 0 \\ 0 & 0 & m_{\beta\alpha} \end{pmatrix} \text{ with } m_{\beta\alpha} = (\rho\phi_\beta, \phi_\alpha)$$

$$A = \begin{pmatrix} B + K_{11} & K_{12} & K_{13} \\ K_{21} & B + K_{22} & K_{23} \\ K_{31} & K_{32} & B + K_{33} \end{pmatrix} \text{ with}$$

$$B = D + K_{11} + K_{22} + K_{33},$$

$$K_{ij} = (K_{ij\beta\alpha}) \text{ with } K_{ij\beta\alpha} = (\eta \frac{\partial \phi_\beta}{\partial x_j}, \frac{\partial \phi_\alpha}{\partial x_i}),$$

$$D = (D_{\beta\alpha}) \text{ with } D_{\beta\alpha} = (\rho u_j \frac{\partial \phi_\alpha}{\partial x_j}, \phi_\beta),$$

$$C_i = (C_{i\beta\alpha}) \text{ with } C_{i\beta\alpha} = (\psi_\gamma, \frac{\partial \phi_\beta}{\partial x_i}).$$

The system of equations (20)-(21) can be written as

$$C_1^T U_1 + C_2^T U_2 + C_3^T U_3 = 0 \tag{22}$$

$$M\dot{\boldsymbol{U}} + A\boldsymbol{U} - CP = 0 \tag{23}$$

By using the backward Euler difference scheme for typical time step $(t_r \rightarrow t_{r+1})$, the system can be reduced to:

$$C_{1_r+1}^T U_1 + C_{2_r+1}^T U_2 + C_{3_r+1}^T U_3 = 0 \tag{24}$$

$$(M + \triangle t_r A)\mathbf{U}_{r+1} + \triangle t_r \bar{C} P_{r+1} = MU_r. \tag{25}$$

Since $A$ in equation (25) depends on $U_{r+1}$, the system is then nonlinear which can be solved by using iterative updating scheme, i.e.,

$$C_{1_r+1}^{Ti+1} U_1 + C_{2_r+1}^{Ti+1} U_2 + C_{3_r+1}^{Ti+1} U_3 = 0 \tag{26}$$

$$(M + \triangle t_r A_{r+1}^i)\mathbf{U}_{r+1}^{i+1} + \triangle t_r \bar{C} P_{r+1}^{i+1} = MU_r^i. \tag{27}$$

where $i$ is the $i^{th}$ iteration step. $\mathbf{U}_1$ and $P_1$ can be determined by $\mathbf{U}_1^0 = \mathbf{U}_0$, $P_1^0 = P_0$, and repeatedly solving the above system until $\|\mathbf{U}_1^{r+1} - \mathbf{U}_1^r\| < \epsilon_u$ and $\|\mathbf{P}_1^{r+1} - \mathbf{P}_1^r\| < \epsilon_p$.

## III. Numerical Results

In this work, we study the flow phenomena of blood in the system of coronary arteries with diseased Left Anterior Descending. The characteristic of the system of coronary arteries is shown in Fig.1. The example under investigation is a coronary system consisting of the base of the aorta, the RCA and the LCA with LAD and LCX. Total volume of the coronary system is 31.1 $cm^3$. The area of aorta inlet surface is 6.712 $cm^2$.

The computational domains used in this study are constructed using a number of CT-images and Mimic software. A three-dimensional system of coronary arteries in stereo-lithography (STL) format has very rough surface which is not suitable for computational fluid dynamic. To smooth its surface, the cubic B-spline interpolation is required.

We simulate the blood flow in the coronary system with different degree of stenosis, 25%, 50% and 75% stenosed artery. The position of the stenosis is at 2.5 $cm$ from the LCA inlet surface. Other parameters are as follows. The density of blood $\rho = 1.06\ g/cm^3$, the infinite shear rate viscosity $\eta_\infty = 0.0345\ (dyne/cm^2) \cdot s$, the zero shear rate viscosity $\eta_0 = 0.56\ (dyne/cm^2) \cdot s$, two model parameters $\lambda = 3.313\ s$ and $n = 0.3568$, the mean pressures $\bar{p}$ of the aorta, the RCA and the LCA are 97, 65, 65 $mmHg$ respectively, and the mean flow rate in the aorta $\bar{Q} = 0.09537\ cm^3 s^{-1}$, and the cardiac period $T = 0.8\ s$.

The boundary value problem presented in section 2 is solved using the Bubnov-Galerkin finite element method via COMSOL Multiphysics. In order to investigate the effect of stenosis on the blood flow as well as on the pressure field and shear rate, three computational domains are constructed for three coronary systems of different degree stenosis. Fig. 2 shows a finite element mesh with a number of Lagrange order two elements.

Fig. 3 shows the vector plot of the velocity field and the sub-domain plot of the pressure of blood in the coronary system having 75% stenosed LAD at the peak of systole. It is noted that blood flows into the system of cornary arteries from the inlet aorta to outlet aorta, the RCA and the LCA. High blood speed and a pressure drop are present around the stenosis arterial section.

To investigate the effect of stenosis on the pressure field, shear rate and mean velocity in the stenosed artery, we consider the numerical results of the pressure field and shear rate at the peak of systole along the LCA axis as shown in Fig.5 and results of mean velocity on the LCA outlet surfaces as shown in Fig.8. The numerical solutions of pressure field and shear rate along the LCA axis and the mean velocity of blood at outlet surfaces of the stenosed LCA are presented in Figs. 6,7 and 9. The results indicate that stenosis of different degrees, namely 25%, 50% and 75%, has a considerable effect on the flow field of blood. It is apparent that a higher degree of stenosis generates a higher pressure and a higher shear rate in the stenosed artery. The mean velocity of blood at three outlet surfaces of the left coronary artery as shown in Fig. 8 is presented. It is observed that the variation of the stenosis degree

reasonably affects the mean velocity instantaneously. The higher the stenosis degree is, the lower mean velocity at the outlet surface of the stenosed vessel is. By increasing the stenosis degree from 25% to 75%, the magnitude of the mean velocity decreases by a remarkable amount, from 22.38 $cm\ s^{-1}$ to 19.50 $cm\ s^{-1}$ at $\Gamma_1^{LAD}$, from 18.53 $cm\ s^{-1}$ to 12.67 $cm\ s^{-1}$ at $\Gamma_s^{LAD}$ and from 25.8 $cm\ s^{-1}$ to 20.83 $cm\ s^{-1}$ at $\Gamma^{LCX}$, as shown in Fig.9.

## IV. Concluding Remarks

A three-dimensional domain of the system of coronary arteries is constructed using MIMIC software and a mathematical model has been developed to study the blood flow in the system of coronary arteries taking into account the pulsatile flow rate and pulse pressure on the inlet and outlet boundaries. The results obtained clearly show that a high blood speed and a pressure drop are found to present in the region next to the throat of stenosis region. With an increase of stenosis degree, the pressure increases and blood velocity deceases. Due to a decrease in blood flow velocity, the blood flow decreases causing not enough blood supply to the heart muscle.

**Acknowledgments:** The first author would like to thank the Development and Promotion of Science and Technology Talents Project (DPST).The last author gratefully acknowledge the support of the Office of the Higher Education Commission and the Thailand Research Fund.

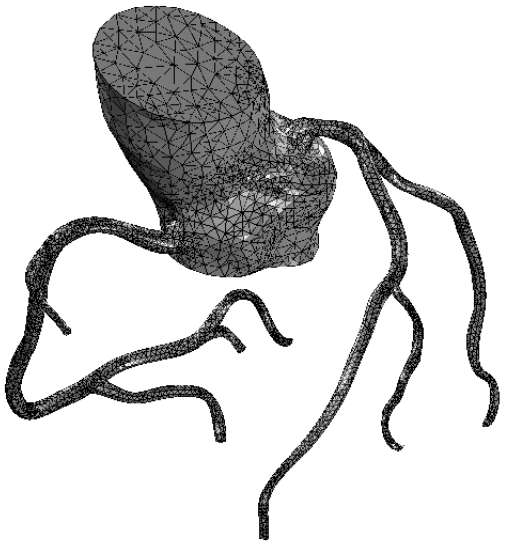

Fig. 2. Domain mesh of a system of coronary arteries.

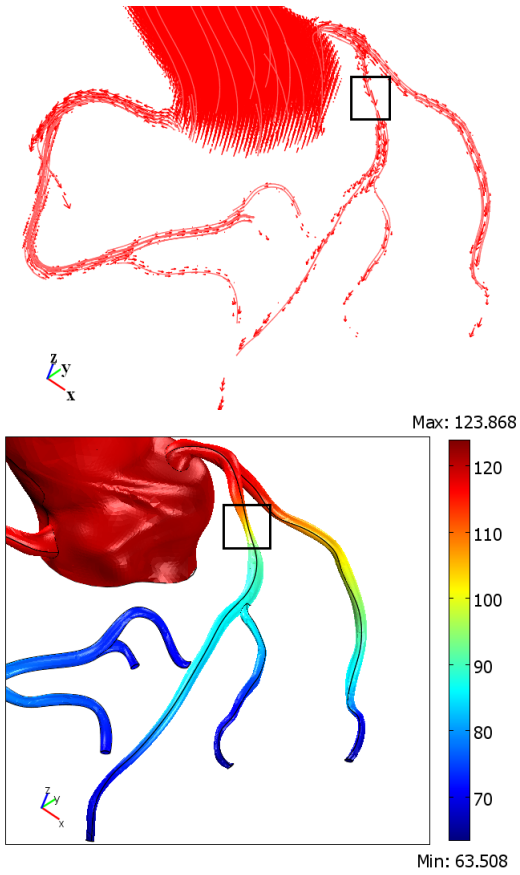


Fig. 3. Velocity and pressure fields at the peak of systole obtained from the model with 75% stenosed LAD

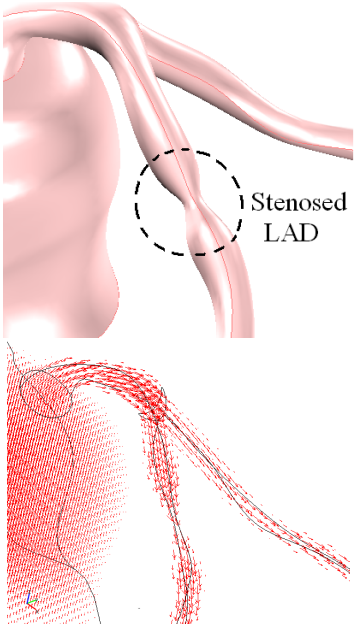


Fig. 4. The 75% stenosed LAD and velocity fields around this area

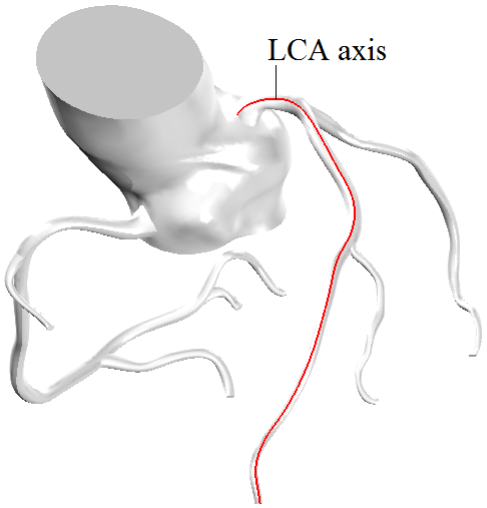


Fig. 5. The system of coronary artery with the investigated arterial axis

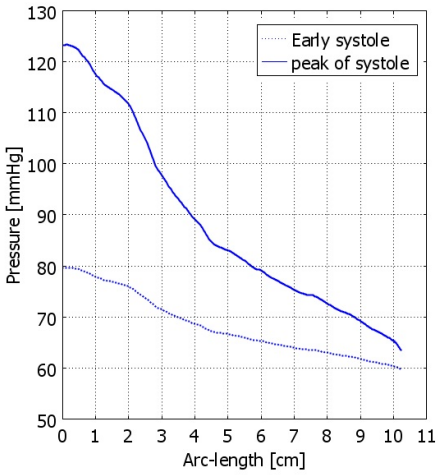


(a)

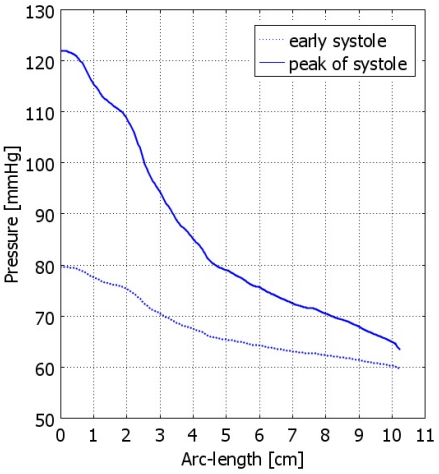


(b)

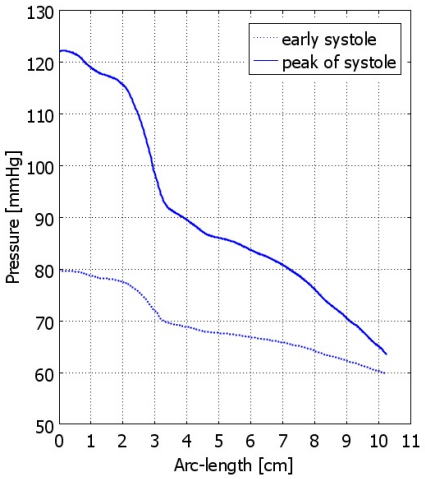


(c)

Fig. 6. Pressure profile along the investigated axis obtained from the model with different degree of stenosis : (a) 25%; (b) 50% and (c) 75%.

## *References:*


[1] T. Ishikawa, L.F.R. Guimaraes, S. Oshima and R. Yamane, Effect of non-Newtonian preperty of blood on flow through a stenosed tube, *Fluid Dynamics Research* vol.2, 1998, pp. 251-264.

[2] A.K. Chaniotis, L. Kaiktsis, D. Katritsis, E. Efstathopoulos, I. Pantos, and V. Marmarellis, Computational study of pulsatile blood flow in prototypevessel geometries of coronary segments, *Physica Medica* vol.26, 2010, pp. 140-156.

[3] S.C.P. Cheung, K.K.L. Wong, G.H. Yeoh, W. Yang, J. Tu, R. Beare and T. Phan, Experimental and numerical study of pulsatile flow through stenosis: Wall shear stress analysis, *Australasian Physical and Engineering Sciences in Medicine* vol.33, 2010, pp. 319-328.

[4] B. Wiwatanapataphee, Modelling of non-Newtonian blood flow through stenosed coronary arteries, *Dynamics of Continuous, Dicrete and Impulsive Systems Series B: Applications & Algorithms* vol.15, 2008, pp. 619-634.

[5] B. Berthier, R. Bouzerar, and C. Legallais, Blood flow patterns in an anatomically realistic coronary vessel: influence of three different reconstruction methods, *Journal of Biomechanics* vol.35, 2002, pp. 1347-1356.

[6] B.M. Johnston, P.R. Johnstona, S. Corney, and D. Kilpatrick, Non-newtonian blood in human right coronary ateries: Steady state simulations, *Journal of Biomechanics* vol.34, 2004, pp. 109-120.

[7] C. Tu and M. Deville, Pulsatile ow of non-newtonian fluids through arterial stenoses, *Journal of Biomechanics* vol.29, 1996, pp. 899-908.

[8] E. Boutsianis, H. Dave, T. Frauenfelder, D. Poulikakos, S. Wildermuth, M. Turina, and G. Zund, Computational simulation of intracoronary flow based on real coronary geometry, *European Journal of Cardio-thoracic Surgery* vol.26, 2004, pp. 248-256.

[9] F.G. Basombrio, E.A. Dari, G.C. Buscaglia and R.A. Feijoo, Numerical experiments in complex hemoynamic ows. non-newtonian effects, *Int.J of Computational Fluid Dynamics* vol.16, 2002, pp. 231-246.

[10] H. Jung, J.W. Choi, and C.G. Park, A symmetric flows of

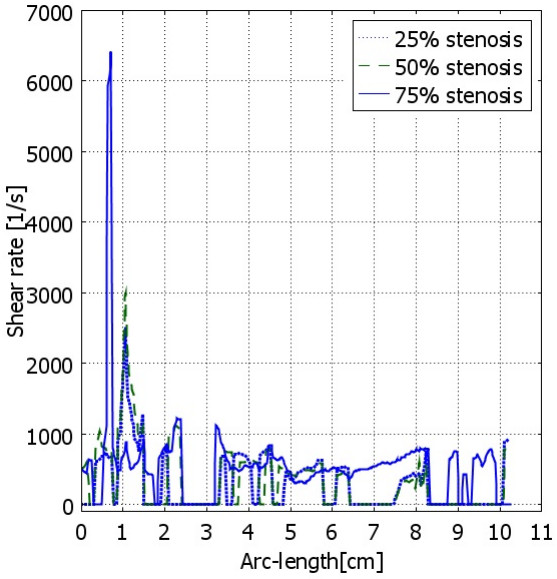


Fig. 7. Shear rate along the investigated axis obtained from the model with different degree of stenosis : 25% (dotted line); 50% (dashed line) and 75% (solid line).

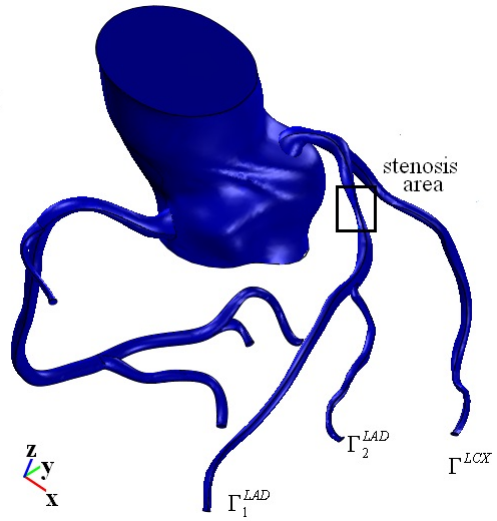


Fig. 8. The system of coronary artery with investigated outlet surfaces $\{\Gamma_1^{LAD}, \Gamma_2^{LAD}, \Gamma^{LCX}\}$ of the left coronary artery.

non-newtonian fluids in symmetric stenosed artery, *Korea-Australia Rheology Journal* vol.16, 2004, pp. 101-108.

[11] J. Chen and X.Y. Lu, Numerical investigation of the non-newtonian blood flow in a bifurcationmodel with a non-planar branch, *Journal of Biomechanics* vol.37, 2004, pp. 1899-1911.

[12] K.S. McCommis, T.A. Glodstein, D.R. Abendschein, B. Missewitz, T. Pilgram, R.J. Gropler, and J. Zheng, Role of myocardial blood volume and flow in coronary artery disease: an experimental mri stdy at rest and during hyperemia, *European Radiology* vol.20, 2010, pp. 2005-2012.

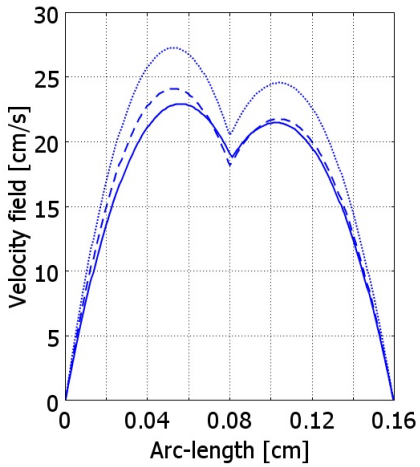


(a)

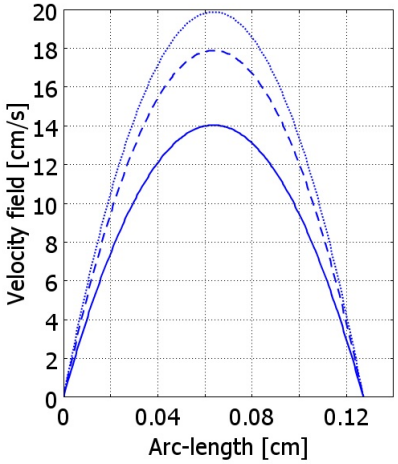


(b)

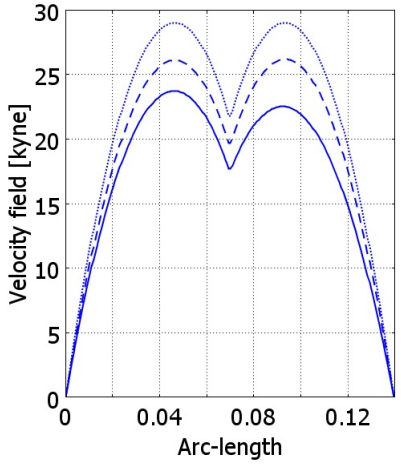


(c)

Fig. 9. Mean velocity obtained from the model with different degree of stenosis : 25% (dotted line); 50% (dashed line) and 75% (solid line) along the diameter of three LCA outlet surfaces: (a) $\Gamma_1^{LAD}$ ; (b) $\Gamma_2^{LAD}$ ; (c) $\Gamma^{LCX}$.

[13] M.M. Zhang, L. Cheng and Y. Zhou, Recent development on fluid-structure interaction control based on surface perturbation. Dynamics of Continuous, *Discrete and Impulsive Systems* vol.14, 2007, pp.467-482.

[14] S.C.P. Cheung, K.K.L. Wong, G.H. Yeoh, W. Yang, J. Tu, R. Beare and T. Phan, Experimental and numerical tudy of pulsatile ow through stenosis: Wall shear stress analysis, *Australasian Physical and Engineering Sciences in Medicine* vol.33, 2010, pp. 319-328.

[15] W. Wiwatanapataphee, D. Poltem, Y.H. Wu and Y. Lenbury, Simulation of pulsatile ow of blood in stenosed coronary artery bypass with graft, *MATHEMATICICAL BIOSCIENCES AND ENGINEERING* vol.3, 2006, pp. 371-383.

[16] W. Yin, S.K. Shanmugavelayudam and D.A. Rubenstein, 3d numerical simulation of coronary blood ow and its effect on endothelial cell activation, *31st Annual International Conference of the IEEE EMBS*, 2009, pp. 4003-4006.

[17] V. Deplano and M. Siooffi, Experimental and numerical study of pulsatile flows through stenosis: wall shear stress analysis, *Jounal of Biomechanics* vol.32, 1999, pp. 1081-1090.

[18] Y.I. Cho and K.R. Kensey, Effects of the non-Newtonian viscosity of blood on flow in a diseased arerial vessel Part 1: Steady flow, *Biorheology* vol.28, 1991, pp. 241-262.

[19] S. Tada and J.M. Tarbell, Flow through internal elastic lamina affects shear stress on smooth muscle cells (3D simulations), *Am J Physiol Heart Circ Physiol* vol.282, 2002, pp. H576-H584.

[20] S. Tada and J.M. Tarbell, Interstital flow through the internal esastic lamina affects share stress on arterial smooth-muscle cells, *Am J Physiol Heart Circ Physiol* vol.278, 2000, pp. H1589-H1597.

[21] S. Tada and J.M. Tarbell, Internal elastic lamina affects the distribution of macromolecules in the arterial wall: A computational study, *Am J Physiol Heart Circ Physiol* vol.287, 2004, pp. H905-H913.

[22] D.K. Stangeby and C.R. Ethier, Computational analysis of coupled blood-wall arterial LDL transpot, *J Biomesh Eng* vol.124, 2002, pp. 1-8.

[23] A.K. Qiao, X.L. Guo, S.G. Wu, Y.J. Zeng and X.H. Xu, Numerical study of nonlinear pulsatile flow in S-shaped curved arteries, *Medical Engineering & Physics* vol.26, 2004, pp. 545-552.

[24] P. Chuchard , B. Wiwatanapataphee , T. Puapansawat and T. Siriapisith, Numerical Simulation of Blood Flow in the System of Human Coronary Arteries with Stenosis, *Proceedings of the 4th WSEAS International Conference on Finite Differences - Finite Elements - Finite Volumes - Boundary Elements* 2011, pp. 59-63.

[25] M. Kang, H.S. Ji and K.C. Kim, An In-vitro investigation of RBCs flow characteristics and hemodynamic feature through a microchanel with a micro-stenosis, *International Journal of Biology and Biomedical Engineering* vol.2, 2008, pp. 1-8.